8th International Symposium on Magnetic Bearing
August 26-28, 2002, Mito, Japan

COMBINED REPETITIVE CONTROL FOR PRECISION RADIAL MAGNETIC BEARING

Xiaoyou Zhang
Graduate School, Tokyo Institute of Technology, Yokohama, 226-8503, Japan
zhangxy44@nano.pi.titech.ac.jp

Tadahiko Shinshi, Lichuan Li and Akira Shimokohbe
Precision & Intelligence Laboratory, Tokyo Institute of Technology, Yokohama, 226-8503, Japan
shinshi@pi.titech.ac.jp

ABSTRACT

The goal of this research is to realize a magnetic bearing which has rotational accuracy of several nanometers at a high speed. To achieve high rotational accuracy, the vibrations of the spindle have to be suppressed. In this paper, first, the vibrations of the spindle are analyzed. The results show that there are two different harmonic vibrations when the spindle is driven by an induction motor. Next, in order to suppress the vibrations, a combined repetitive control method, which includes two types of repetitive compensators, is proposed. Furthermore, the effectiveness of the proposed method for suppressing the vibrations is verified through experiments and the experimental results show the rotational accuracy is improved from 301.2 nm (3σ) to 21.9 nm at 2,880 min^{-1}.

INTRODUCTION

Magnetic bearings can compensate for spindle motion errors caused by spindle unbalance and disturbance forces because of their active motion control capability. Moreover the magnetic bearings are free from friction and can be used in a vacuum so that they can be candidates for high accurate and high-speed bearings in the future [1]. However the rotational accuracy of conventional magnetic bearings is down to the micron level. Few magnetic bearings of nanometer rotational accuracy have been reported. The goal of this research is to realize a magnetic bearing which has rotational accuracy of several nanometers at a high speed.

To realize a magnetic bearing with high rotational accuracy, the vibrations of the spindle have to be suppressed. One vibration source is unbalance force caused by the mismatch between the profile and the inertia centers of the spindle. Another vibration source is excitation force of the electromagnets caused by the mismatch between the geometric centers of the sensor target and the electromagnet target. These vibrations depend on the rotational frequency of the spindle. They can be suppressed by a conventional repetitive controller which generates a periodic signal of the rotational frequency [2-4].

To rotate the spindle at a high speed, a high-speed induction motor is commonly used. The motor produces radial unbalanced magnetic pull (UMP) because of eccentricity [5]. Therefore the motor becomes an additional vibration source to the spindle. The vibrations generated by the motor are dependent on the rotational frequency of the spindle and the fundamental frequency of the motor current [6, 7].

When the induction motor is used to rotate the spindle, the rotational frequency of the spindle is different from the fundamental frequency of the motor current because of motor slip. In this case, there are two different harmonic vibrations on the spindle. Because the conventional repetitive controller has a repetitive compensator (signal generator) dependent on the rotational frequency, the vibrations dependent on the fundamental frequency of the motor current cannot be suppressed, preventing further improvement of the rotational accuracy.

This paper presents a control method for improving the rotational accuracy of the magnetic bearing under the consideration of the UMP of the motor. First, in order to understand factors affecting the rotational accuracy, the vibrations of the spindle are analyzed. Next, a combined repetitive control method, which includes two types of repetitive compensators, is proposed. Furthermore, the effectiveness of the proposed method for improving the rotational accuracy is verified through experiments.

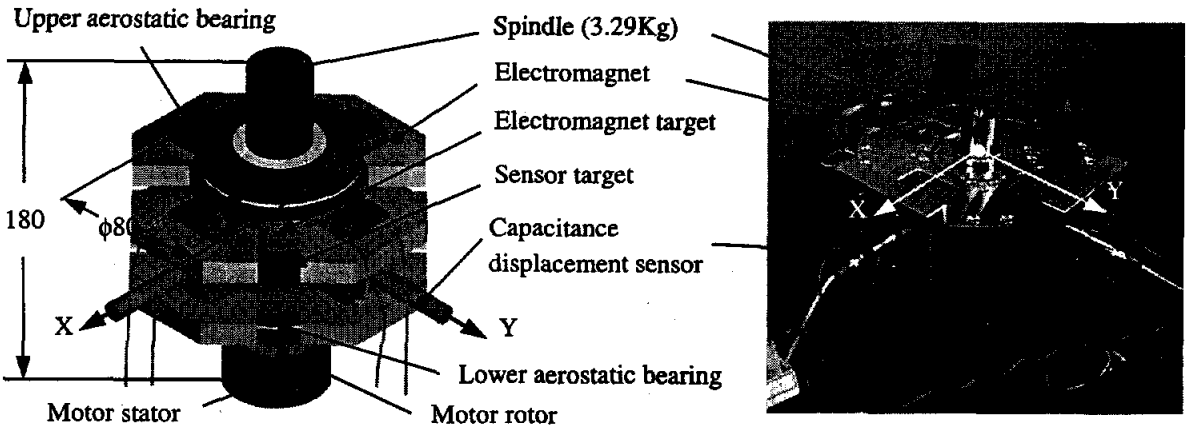

FIGURE 1: Schematic of radial magnetic bearing (In photograph, upper aerostatic bearing is not assembled)

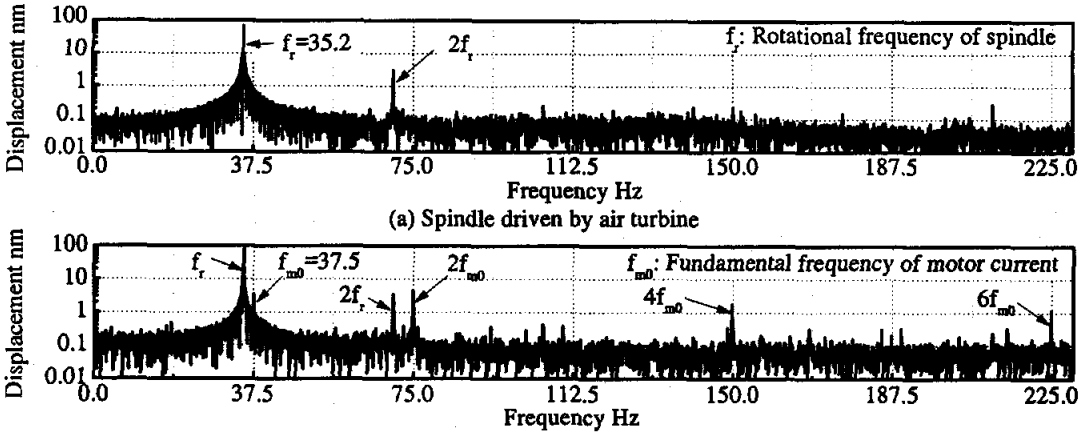

(a) Spindle driven by air turbine

(b) Spindle driven by induction motor

FIGURE 2: FFT analysis of spindle displacement in X direction at 2,110 min^{-1}

SPINDLE VIBRATION ANALYSIS

Experimental magnetic bearing

An experimental radial magnetic bearing is shown Figure 1. The spindle motions in the radial direction are controlled by eight electromagnets. The translational motion in the direction of gravity and tilting motions of the spindle are constrained by upper and lower aerostatic bearings. The displacements of the spindle in the radial direction are measured by two capacitance displacement sensors (Microsense II 5130, ADE, measurement range ±0.1 mm). The roundness of the sensor target centered in the spindle is 30 nm. The mass of the spindle is 3.29 kg and the maximum diameter is 80 mm. The spindle can be alternatively driven by an air turbine or a 3-phase 2-pole induction motor (0.1kW TBO-K 2P, Hitachi) and an inverter (SJ100-002LFR, Hitachi). The magnetic bearing is controlled via a digital signal processor (DS1103 PPC Controller Board, dSPACE). In this paper, only radial motion accuracies are discussed.

Measurement of spindle vibration

Figure 2 shows the FFT analysis results of the displacements of the spindle in the X direction (shown in Figure 1) at 2,100 min^{-1} when the spindle is driven by the air turbine or the induction motor. When the spindle displacements are measured, a controller suppressing periodic disturbances is not implemented.

When the spindle is driven by the air turbine, the vibrations of the spindle included the rotational frequency f_r and its second harmonic $2f_r$ (f_r = 35.2 Hz), as shown in Figure 2(a). However when the spindle is driven by the induction motor, the vibrations included not only the rotational frequency f_r and its second harmonic $2f_r$, but also the fundamental frequency of the motor current f_{m0} and its harmonics $2f_{m0}$, $4f_{m0}$, $6f_{m0}$ (f_{m0} = 37.5 Hz), as shown in Figure 2(b).

Analysis of excitation forces acting on spindle

Unbalance force of spindle. Generally, the profile center and the inertia center of the spindle are not aligned. When the spindle rotates at the profile center (geometric center of sensor target), an unbalance force is produced synchronized with the spindle rotation. The

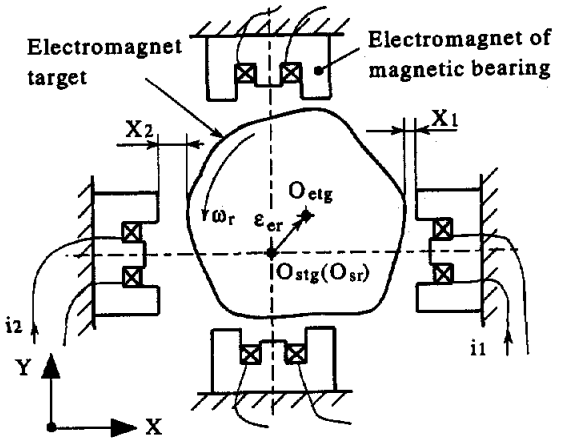

FIGURE 3: Eccentricity of electromagnet target

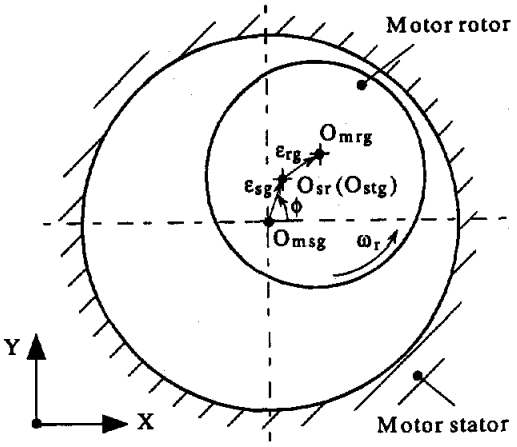

FIGURE 4: Eccentricity of motor

unbalance force generates the vibration of frequency f_r.

Excitation force of electromagnets. The geometric center of the electromagnet target O_{etg} has an eccentricity ε_{er} with respect to the geometric center of the sensor target O_{stg}, as shown in Figure 3. Furthermore, there is a profile error in the electromagnet target.

When the spindle rotates at the geometric center of the sensor target O_{stg}, the air gaps of electromagnets change due to the eccentricity and the profile error of the electromagnet target. Therefore excitation forces are produced by the electromagnets. The excitation forces are dependent on the rotational frequency and generate the vibrations of frequency f_r and its harmonics.

UMP of motor. The rotational center of the spindle O_{sr} (O_{stg}) has an eccentricity ε_{sg} with respect to the geometric center of the motor stator O_{msg}. Furthermore, the geometric center of the motor rotor O_{mrg} has an eccentricity ε_{rg} with respect to the rotational center O_{sr} (O_{stg}), as shown in Figure 4. Additionally, because the motor is driven by the inverter, various frequencies are included in the motor current.

The UMP in X direction generated by the eccentricity and the motor current is given as [7]

$$
\begin{aligned}
F_{mx}(t) = K\cdot\{&2\sum_{j=0}^{\infty} I_{mj}^2\cdot[\varepsilon_{sg}\cos\phi+\varepsilon_{rg}\cos\omega_r t]\\
&+\sum_{j=0}^{\infty} I_{mj}^2[\varepsilon_{sg}\cos(2\omega_{mj}t-\phi+2\alpha_j)\\
&\quad+\varepsilon_{rg}\cos[(2\omega_{mj}-\omega_r)t+2\alpha_j]]\\
&+2\sum_{j=0}^{\infty}\sum_{k=j+1}^{\infty} I_{mj}I_{mk}[\varepsilon_{sg}\cos[(\omega_{mj}+\omega_{mk})t-\phi+\alpha_j+\alpha_k]\\
&\quad+\varepsilon_{rg}\cos[(\omega_{mj}+\omega_{mk}-\omega_r)t+\alpha_j+\alpha_k]]\\
&+2\sum_{j=0}^{\infty}\sum_{k=j+1}^{\infty} I_{mj}I_{mk}[\varepsilon_{sg}\cos[(\omega_{mj}-\omega_{mk})t+\phi+\alpha_j-\alpha_k]\\
&\quad+\varepsilon_{rg}\cos[(\omega_{mj}-\omega_{mk}+\omega_r)t+\alpha_j-\alpha_k]]\\
&+2\sum_{j=0}^{\infty}\sum_{k=j+1}^{\infty} I_{mj}I_{mk}[\varepsilon_{sg}\cos[(\omega_{mj}-\omega_{mk})t-\phi+\alpha_j-\alpha_k]\\
&\quad+\varepsilon_{rg}\cos[(\omega_{mj}-\omega_{mk}-\omega_r)t+\alpha_j-\alpha_k]]\}
\end{aligned}
\tag{1}
$$

Where, K is a constant, j is zero or a positive integer, k is a positive integer, I_{mj} (or I_{mk}), α_j (or α_k) and ω_{mj} (or ω_{mk}) are the amplitude, phase angle, and angular velocity of various components of the motor current, ω_r is the angular speed of the spindle, and ϕ is the angle of the eccentricity ε_{sg} with respect to the X axis.

From Equation (1), it can be seen that the UMP has such frequencies as (1) the spindle rotational frequency component f_r ($f_r = \omega_r/2\pi$), (2) the multiple components of various frequencies of the motor current $2f_{mj}$ ($f_{mj} = \omega_{mj}/2\pi$), (3) the combined components of various frequencies of the motor current and the rotational frequency of the spindle $2f_{mj} - f_r$, $f_{mj} + f_{mk} - f_r$ and $f_{mj} - f_{mk} \pm f_r$ ($j \neq k$; $f_{mk} = \omega_{mk}/2\pi$), and (4) the combined components of various frequencies of the motor current $f_{mj} \pm f_{mk}$ ($j \neq k$). The vibrations generated by the UMP of the induction motor include not only the component depending on the rotational frequency of the spindle f_r, but also the components depending on the fundamental frequency of the motor current, such as f_{m0}, $2f_{m0}$, $4f_{m0}$ and $6f_{m0}$.

The vibration of frequency f_{m0} is believed to be produced by the UMP of the combined components of various frequencies of the motor current and the rotational frequency of the spindle, as shown in the eighth term of Equation (1). The eighth term of Equation (1) can be rewritten as

$$
\begin{aligned}
F_{mx-8}(t) = 2K\cdot\sum_{j=0}^{\infty}\sum_{k=j+1}^{\infty} I_{mj}I_{mk}\varepsilon_{rg}\\
\cdot\cos[2\pi(f_{mj}-f_{mk}+f_r)t+\alpha_j-\alpha_k]
\end{aligned}
\tag{2}
$$

The vibrations of frequencies $2f_{m0}$, $4f_{m0}$ and $6f_{m0}$ are believed to be produced by the square of the frequency of the motor current (the third term of Equation (1)) or a combination of different frequencies of the motor current (The fifth, seventh and ninth terms of Equation (1)). The third, fifth, seventh and ninth terms of Equation (1) can be rewritten as

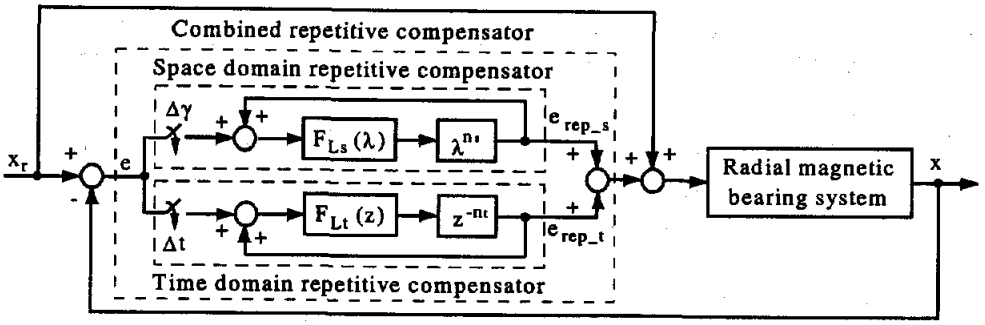

FIGURE 5: Block diagram of combined repetitive control system

$$F_{mx-3}(t) = K \cdot \sum_{j=0}^{\infty} I_{mj}^2 \varepsilon_{sg} \cos[2\pi(2f_{mj})t - \phi + 2\alpha_j] \quad (3)$$

$$F_{mx-5}(t) = 2K \cdot \sum_{j=0}^{\infty} \sum_{k=j+1}^{\infty} I_{mj} I_{mk} \varepsilon_{sg} \cdot \cos[2\pi(f_{mj} + f_{mk})t - \phi + \alpha_j + \alpha_k] \quad (4)$$

$$F_{mx-7}(t) = 2K \cdot \sum_{j=0}^{\infty} \sum_{k=j+1}^{\infty} I_{mj} I_{mk} \varepsilon_{sg} \cdot \cos[2\pi(f_{mj} - f_{mk})t + \phi + \alpha_j - \alpha_k] \quad (5)$$

$$F_{mx-9}(t) = 2K \cdot \sum_{j=0}^{\infty} \sum_{k=j+1}^{\infty} I_{mj} I_{mk} \varepsilon_{sg} \cdot \cos[2\pi(f_{mj} - f_{mk})t - \phi + \alpha_j - \alpha_k] \quad (6)$$

COMBINED REPETITIVE CONTROL

Scheme of combined repetitive control system

When the spindle is rotated by the induction motor, the spindle vibrations of the two different fundamental frequencies (f_r and f_{m0}) and their harmonics ($2f_r$ and $2f_{m0}$, $4f_{m0}$, $6f_{m0}$) are both produced, as shown in Figure 2 (b). The conventional repetitive controller [2-4] has only one signal generator (repetitive compensator) in the control loop. It is effective to suppress the vibrations of only one fundamental frequency and its harmonics.

A repetitive control system that includes multiple repetitive compensators with different periods is needed to suppress the vibrations of both the fundamental frequencies and their harmonics. Therefore, in this paper, a combined repetitive control is proposed, as shown in Figure 5. The combined repetitive controller includes two types of repetitive compensators. One is a space domain repetitive compensator. The space domain repetitive compensator generates a periodic signal related to the rotational angle of the spindle to suppress the vibrations dependent on the rotational frequency of the spindle. The other is a time domain repetitive compensator. The time domain repetitive compensator generates a periodic signal related to the fundamental period of the motor current to suppress the vibrations dependent on the fundamental frequency of the motor current.

Combined repetitive compensator

To stabilize the repetitive control system, low-pass filters $F_{Ls}(\lambda)$ and $F_{Lt}(z)$ are introduced, as shown in Figure 5. The λ and z^{-1} are delay elements. The λ corresponds to one step of one period of the spindle rotation divided by the sampling angle $\Delta\gamma$. The z^{-1} corresponds to one sampling time Δt obtained by dividing the fundamental period of the motor current.

The $F_{Ls}(\lambda)$ is a linear-phase filter and is made up of some delay elements of the repetitive compensator. The cutoff frequency of the filter is related to the spindle rotational speed. To keep the fixed cutoff frequency of the filter, reset of the coefficients of the filter is necessary at different rotational speeds. However, reset of the coefficients increases the complexity of the control algorithm. To simplify the control algorithm, the filter is designed at any rotational speed and used at all rotational speeds. Therefore, the $F_{Ls}(\lambda)$ is a filter that has a changed cutoff frequency at different rotational speeds. The design method of the filter $F_{Lt}(z)$ is the same as that used to design the filter $F_{Ls}(\lambda)$.

In our research, the delay steps of the space domain and the time domain repetitive compensators are selected to be 158 and 100, respectively. The sampling angle $\Delta\gamma$ of the space domain repetitive compensator is 0.04 rad. The sampling time Δt of the time domain repetitive compensator is 0.2 ms when the fundamental frequency of the motor current is 50.0 Hz. The orders of the filters $F_{Ls}(\lambda)$ and $F_{Lt}(z)$ are set to be 16, respectively. The coefficients of the filter $F_{Ls}(\lambda)$ are set at 1,200 min^{-1} and the cutoff frequency is 250 Hz. The coefficients of the filter $F_{Lt}(z)$ are set when the fundamental frequency of the motor current is 50.0 Hz and the cutoff frequency is 450 Hz.

EXPERIMENTAL RESULTS

Controller types

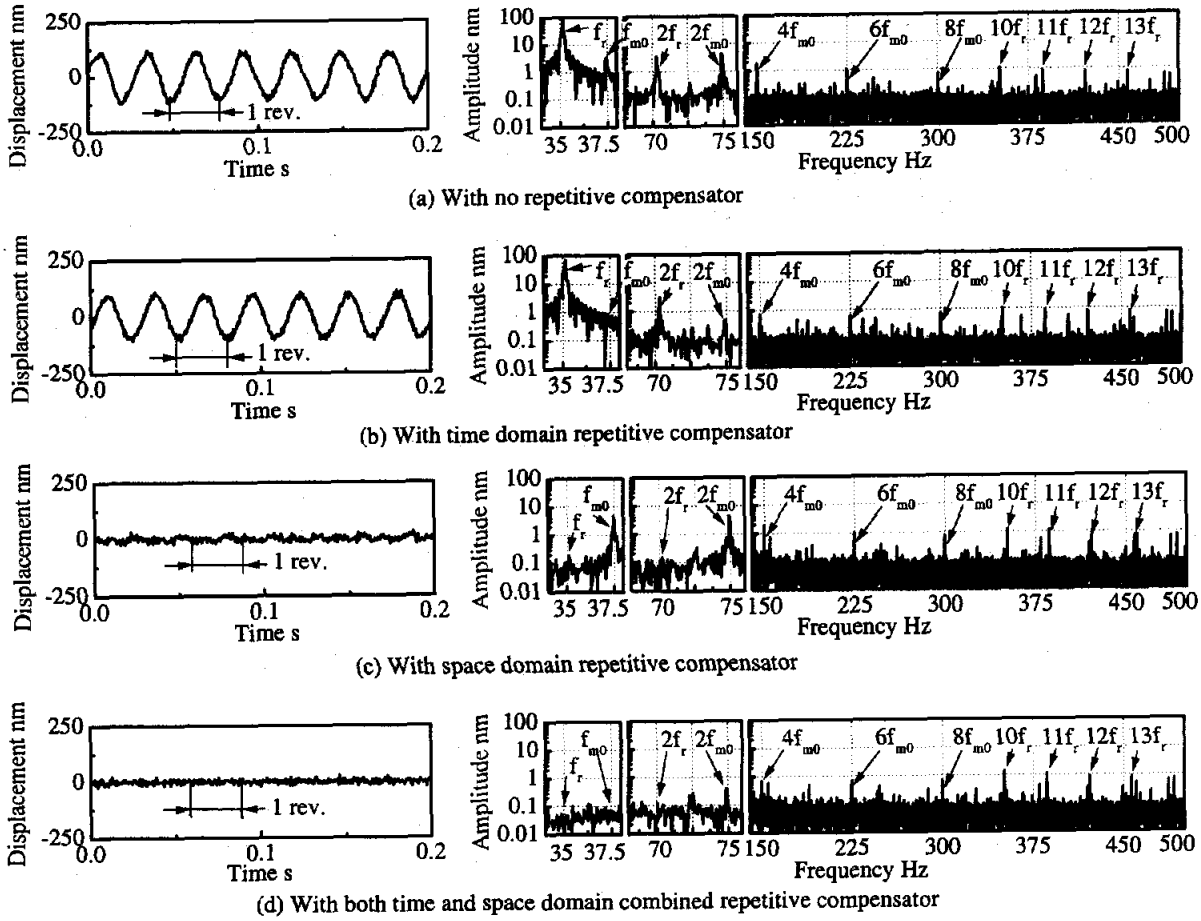

FIGURE 6: Displacements of spindle in X direction at 2,110 min^{-1}

To evaluate the effectiveness of the combined repetitive control, four types of controller; (1) no repetitive compensator, (2) a time domain repetitive compensator, (3) a space domain repetitive compensator and (4) both time and space domain combined repetitive compensator are applied to the experimental radial magnetic bearing and the rotational accuracies of the four controllers are compared.

Displacements of spindle

Figure 6 shows the displacements of the spindle in the X direction and the FFT analysis results under each of control systems, at 2,110 min^{-1}. The displacements are the same in the Y direction, and those results are not shown in Figure 6.

Comparing Figure 6(a) with Figure 6(b), using the time domain repetitive compensator alone, the vibrations (f_{m0}, $2f_{m0}$, $4f_{m0}$ and $6f_{m0}$) dependent on the fundamental frequency of the motor current are reduced, but the vibrations (f_r and $2f_r$) dependent on the rotational frequency of the spindle could not be suppressed. On the contrary, as shown in Figure 6(c), using the space domain repetitive compensator alone, the vibrations dependent on the rotational frequency of the spindle are reduced, but the vibrations dependent on the fundamental frequency of the motor current could not be suppressed.

As shown in Figure 6(d), the combination of both the time and space domain repetitive compensators reduced all the vibrations dependent on the rotational frequency of the spindle and the fundamental frequency of the motor current under the frequency of approximately 250 Hz. However, this method is less effective in suppressing the vibrations of the frequency over approximately 250 Hz. One reason is that the bandwidth (approximately 250 Hz) of the magnetic bearing system is limited. Another reason may be that the fundamental frequency of the motor current changes slightly during the control because of instability of the inverter. In other words, the fundamental period of the given motor current does not match the period of the function generated by the time domain repetitive compensator and their difference may increase as the order of harmonic of the vibration increases. Comparing Figure 6(c) with Figure 6(d), obvious difference of the time series cannot be seen. The reason is that the

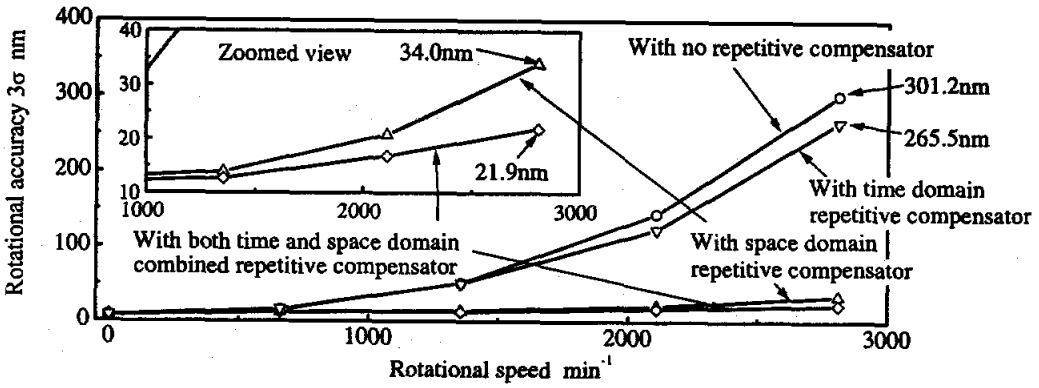

FIGURE 7: Rotational accuracies

vibrations of the frequency over approximately 250 Hz are not suppressed.

Rotational accuracy

Figure 7 shows the rotational accuracies (3σ) under each of control systems at various rotational speeds. The standard deviation σ is calculated from the time series of the displacement e_r in the radial direction.

$$e_r = \sqrt{x^2 + y^2} \tag{7}$$

Where x and y are the output of the displacement sensors in the X and Y directions. The effectiveness of the combined repetitive control is clearly demonstrated for improving the rotational accuracy of the spindle in total rotation ranges. For example, at 2,880 min^{-1}, the rotational accuracy is 301.2 nm (3σ) without repetitive compensator, 265.5 nm with the time domain repetitive compensator alone, 34.0 nm with the space domain repetitive compensator alone, and 21.9 nm with the combined repetitive compensator.

CONCLUSIONS

In order to suppress the vibrations induced by the unbalanced magnetic pull (UMP) of the induction motor, a combined repetitive control method was proposed. The combined repetitive control could reduce the vibrations dependent on the rotational frequency of the spindle and the fundamental frequency of the motor current. The rotational accuracy of the spindle was improved by the combined repetitive control from 301.2 nm (3σ) to 21.9 nm at 2,880 min^{-1}.

The future works are to suppress the vibrations of the frequency over 250 Hz and reduce the motor current noises from the inverter.

ACKNOWLEDGEMENTS

This research was supported in part by a research grants from the Ministry of Education and Science, and Electro Mechanic Technology Advancing Foundation.

References

1. T. Shinshi, C. Iijima, X. Zhang, K. Choi, K. Sato and A. Shimokohbe: Precision Radial Magnetic Bearing, Proceedings of ASPE 15th Annual Meeting, Arizona, U.S.A., (2000) 240.
2. K. Karino, B. Nagai and Y. Okada: Repetitive Control of Magnetic Bearing, Transactions of the Japan Society of Mechanical Engineers, C, 62, 12 (1996) 4580, (in Japanese).
3. M. Nakano, J. She and Y. Matsuo: A New Approach to Reject Angle Dependent Disturbances in Constant Speed Rotation Control Systems, JAPAN/USA Symposium on Flexible Automation, San Francisco, (1992) 151.
4. X. Zhang, T. Shinshi, L. Li, K. Choi and A. Shimokohbe: Precision Control of Radial Magnetic Bearing, 10th International Conference on Precision Engineering (ICPE), Yokohama, Japan, (2000) 714.
5. S. Yang: Low-noise Electrical Motor, Clarendon Press, Oxford, 1981.
6. H. Kanzaki, J. Shibayama, S. Watanabe, M. Ichimonji and M. Namiki: Unstable Electrical Vibration of an Induction Motor, Transactions of the Japan Society of Mechanical Engineers, C, 60, 10 (1994) 3238, (in Japanese).
7. X. Zhang, T. Shinshi, L. Li and A. Shimokohbe: A Combined Repetitive Control for Precision Rotation of Magnetic Bearing, Submitted to Precision Engineering.